Received: 27 September 2022 | Revised: 17 January 2023 | Accepted: 7 February 2023

DOI: 10.1002/pro.4592

FULL-LENGTH PAPER

THE PROTEIN SOCIETY WILEY

FkpA enhances membrane protein folding using an extensive interaction surface

Taylor Devlin | **Dagan C. Marx** | **Michaela A. Roskopf** | **Quenton R. Bubb** | **Ashlee M. Plummer** | **Karen G. Fleming**

T.C. Jenkins Department of Biophysics, Johns Hopkins University, Baltimore, Maryland, USA

Correspondence
Karen G. Fleming, T.C. Jenkins Department of Biophysics, Johns Hopkins University, Jenkins Hall, 3400 N. Charles Street, Baltimore, MD 21218-2685, USA.
Email: karen.fleming@jhu.edu

Funding information
National Institute of General Medical Sciences, Grant/Award Number: T32-GM008403; National Science Foundation, Grant/Award Numbers: DGE 1232825, MCB 1931211

Review Editor: Aitziber L. Cortajarena

Abstract

Outer membrane protein (OMP) biogenesis in gram-negative bacteria is managed by a network of periplasmic chaperones that includes SurA, Skp, and FkpA. These chaperones bind unfolded OMPs (uOMPs) in dynamic conformational ensembles to suppress aggregation, facilitate diffusion across the periplasm, and enhance folding. FkpA primarily responds to heat-shock stress, but its mechanism is comparatively understudied. To determine FkpA chaperone function in the context of OMP folding, we monitored the folding of three OMPs and found that FkpA, unlike other periplasmic chaperones, increases the folded yield but decreases the folding rate of OMPs. The results indicate that FkpA behaves as a chaperone and not as a folding catalyst to influence the OMP folding trajectory. Consistent with the folding assay results, FkpA binds all three uOMPs as determined by sedimentation velocity (SV) and photo-crosslinking experiments. We determine the binding affinity between FkpA and $uOmpA_{171}$ by globally fitting SV titrations and find it to be intermediate between the known affinities of Skp and SurA for uOMP clients. Notably, complex formation steeply depends on the urea concentration, suggesting an extensive binding interface. Initial characterizations of the complex using photo-crosslinking indicate that the binding interface spans the entire FkpA molecule. In contrast to prior findings, folding and binding experiments performed using subdomain constructs of FkpA demonstrate that the full-length chaperone is required for full activity. Together these results support that FkpA has a distinct and direct effect on OMP folding that it achieves by utilizing an extensive chaperone-client interface to tightly bind clients.

KEYWORDS

FkpA, membrane protein folding, outer membrane protein, outer membrane protein biogenesis, periplasmic chaperone, photo-crosslinking, sedimentation velocity

1 | INTRODUCTION

The outer membrane of gram-negative bacteria serves as the first line of defense against extracellular threats, and outer membrane biogenesis and stability are essential for cell viability (Masuda et al., 2009). The outer membrane is composed of lipids and outer membrane proteins (OMPs) that facilitate the flux of small molecules, maintain membrane integrity, and promote virulence in pathogenic strains. To fold into the outer membrane, an OMP must first traffic across multiple cellular compartments in an unfolded but folding-competent conformation (Plummer and Fleming, 2016). Unfolded OMPs (uOMPs) are translated in the cytoplasm and post-translationally translocated into the aqueous periplasm through the Sec YEG translocon (Silhavy et al., 2006). Because uOMPs contain highly hydrophobic regions and otherwise readily aggregate in water (Danoff and Fleming, 2015; Tan et al., 2010), they are bound and released by a network of periplasmic chaperones to prevent off-pathway aggregation before folding into the outer membrane is catalyzed by the β-barrel assembly machine (BAM) (Costello et al., 2016; Plummer and Fleming, 2016). Importantly, all of these processes must occur in the absence of ATP (Wülfing and Plückthun, 1994) and be primed to respond to changing environmental conditions that could occur as a consequence of the leaky outer membrane. How do periplasmic chaperones suppress uOMP aggregation and promote native folding in the absence of an external energy source and in the face of external stress? Understanding the general principles governing these ATP-independent chaperone-client interactions contributes to the growing comprehension of bacterial protein homeostasis in virulent strains and informs the development of antibiotics targeting the cell envelope.

Major players in the OMP biogenesis chaperone network include SurA, Skp, and FkpA with additional contributions from Spy and the protease chaperone DegP (Figure 1) (He et al., 2021; Missiakas et al., 1996). While much of the recent work elucidating the mechanisms of these ATP-independent chaperones focuses on the chaperones SurA and Skp (Burmann et al., 2013; Calabrese et al., 2020; Holdbrook et al., 2017; Humes et al., 2019; Jia et al., 2020; Marx et al., 2020a, 2020b; Mas et al., 2020; Pan et al., 2020; Sandlin et al., 2015; Schiffrin et al., 2017; Thoma et al., 2015), thermodynamic and mechanistic information about the function of FkpA in OMP biogenesis remains sparse (Ge et al., 2014; Ruiz-Perez et al., 2010). Structurally, FkpA forms homodimers and comprises two domains: an N-terminal, α-helical domain that mediates dimerization and a C-terminal domain homologous to FK506-binding proteins and capable of catalyzing peptidyl-prolyl isomerization (PPIase) reactions (Arie et al., 2001; Bothmann and Plückthun, 2000; Ramm and Plückthun, 2001; Saul et al., 2004). The structural domains are connected by a long and flexible α-helix, allowing the two C-terminal domains to move independently of each other (Hu et al., 2006; Olsson et al., 2015; Saul et al., 2004). There are unstructured tails at both the N- and C- termini, but these intrinsically disordered regions have not been ascribed any functional importance (Hu et al., 2004; Saul et al., 2004).

FkpA manifests its chaperone function by increasing the solubility and decreasing aggregation of a variety of unfolded or misfolded proteins (primarily non-OMPs) *in vitro* (Arie et al., 2001; Bothmann and Plückthun, 2000; Hu et al., 2006; Ramm and Plückthun, 2000, 2001; Saul et al., 2004). Additionally, FkpA improves yields of recombinantly expressed proteins when co-expressed in the same system (Bothmann and Plückthun, 2000; Cumby

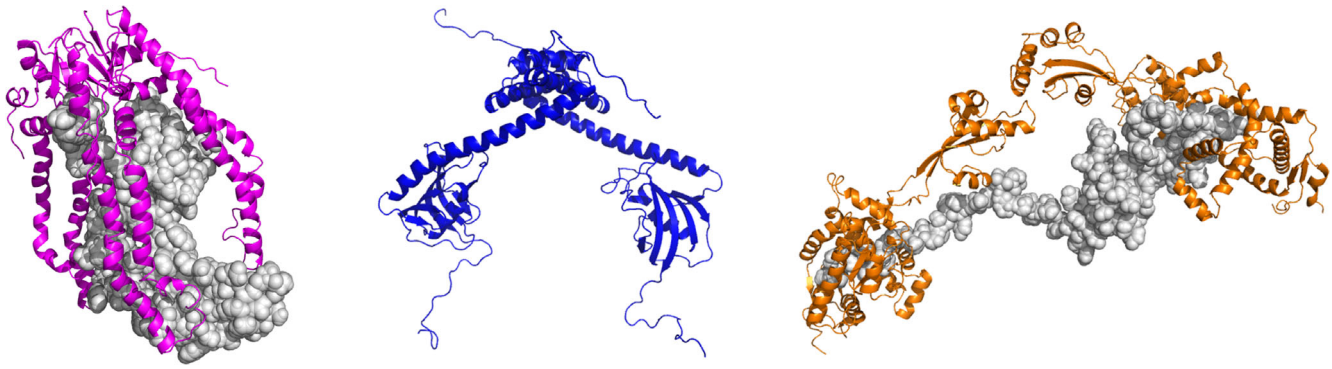

FIGURE 1 Three periplasmic chaperones involved in OMP biogenesis. Well studied periplasmic chaperones Skp (left, pink) and SurA (right, orange) use distinct mechanisms to chaperone unfolded outer membrane proteins in the periplasm, and models of each complex have been published. By contrast, limited information about the mechanism and chaperone-client complex is available for FkpA (middle, blue). The dimeric structure of FkpA was created from PDB 1Q6U (Saul et al., 2004) with the N- and C-terminal tails added in PyMol (DeLano, 2015). The model of Skp binding $uOmpA_{171}$ is modified from Zaccai et al. (2016). The model of multiple SurA molecules binding an extended $uOmpA_{171}$ is modified from Marx et al. (2020b).

et al., 2015; Dwyer et al., 2014; Gunnarsen et al., 2010, 2013; Padiolleau-Lefèvre et al., 2006). In the context of OMP biogenesis, FkpA rescues *ΔsurA Δskp* lethality at elevated temperatures (Ge et al., 2014) and is upregulated by the *E. coli* sigma E (σ^E) stress response (Danese and Silhavy, 1997; Rhodius et al., 2006), implying this chaperone contributes as an important mitigator of increased uOMP aggregation risk in the periplasm under stress conditions. Due to the redundant and functionally overlapping nature of the OMP biogenesis chaperone network, FkpA is not essential to cell survival, but cumulative data suggest that it is a potent stress-response chaperone with a wide range of possible OMP and non-OMP clients.

Despite evidence for FkpA exhibiting chaperone function on model unfolded or misfolded proteins both *in vivo* and *in vitro*, limited information is available about FkpA binding to physiologically relevant OMPs (Ge et al., 2014; Ruiz-Perez et al., 2010). It is also not known how FkpA influences the folding trajectory of uOMPs. Here we address these questions using the transmembrane β-barrel of outer membrane protein A ($OmpA_{171}$), OmpX, and BamA as unfolded clients to study both the chaperone function and binding affinity of FkpA. The full-length and dimeric FkpA exhibits chaperone function in an OMP folding assay by increasing the total folded population of all three OMPs and reducing the rate of $OmpA_{171}$ and OmpX folding. This chaperone activity is distinct from the effects of periplasmic chaperones SurA or Skp. FkpA binds all three OMP clients and clearly prevents BamA aggregation in sedimentation velocity analytical ultracentrifugation (SV-AUC) experiments. Furthermore, we observe a steep urea-dependence of the binding constant indicating that a large surface area is buried upon client binding. We find the FkpA binding affinity for uOMPs to be in the low nM range in the absence of denaturant, which is more favorable than that of SurA but less favorable than that of Skp based on direct competition for $uOmpA_{171}$ binding. Site specific photo-crosslinking between FkpA and a uOMP complements the urea dependence of the binding constant by showing that the interaction interface spans both structural domains of FkpA. We hypothesize that dimerization mediated by the N-domain brings the two PPIase domains into close proximity to create an extensive binding surface with much higher affinity for unfolded or misfolded clients.

2 | RESULTS

2.1 | FkpA increases the folding yield but slows the folding rate of OMPs

We investigated the function of FkpA (FkpA refers to the full-length, dimeric form of the protein unless otherwise stated) by observing its effect on the folding of three different OMPs: the β-barrel domain of OmpA($OmpA_{171}$), outer membrane protein X (OmpX), and β-barrel assembly machine A (BamA). $OmpA_{171}$ and OmpX represent small, 8-stranded β-barrels abundant in the *E. coli* outer membrane while BamA is a an essential 16-stranded β-barrel (Figure S1). The folding of all three have been previously studied (Kleinschmidt et al., 1999; Danoff and Fleming, 2017; Burgess et al., 2008). We take advantage of the heat-modifiability of folded OMPs in mixed SDS-phospholipid micelles to separate folded and unfolded populations into distinct bands on an SDS-PAGE gel that can be quantified by densitometry (Burgess et al., 2008; Kleinschmidt and Tamm, 1996, 2002; Nakamura and Mizushima, 1976; Pocanschi et al., 2006; Surrey and Jahnig, 1995). As has been demonstrated previously in the literature, the folded and unfolded fractions do not add to unity due to the presence of an elusive state that migrates anomalously on a polyacrylamide gel (Danoff and Fleming, 2017). Therefore, a fraction elusive was also quantified. The exact nature of this elusive state is unknown, but $OmpA_{171}$ has been shown to form unfolded oligomers in the presence of lipids or detergents (Wang et al., 2013). We interpret that the elusive state represents off-pathway, lipid-induced aggregates since this phenomenon does not occur in the absence of lipids (Danoff and Fleming, 2017). Full details are provided in Supplemental Section "Methods".

In the absence of chaperone, roughly 50% of the total $OmpA_{171}$ folds into 1,2-diundecanoyl-$_{sn}$-glycero-3-phosphocholine ($diC_{11}PC$) large unilamellar vesicles (LUVs) after 1 h (Figures 2a and S2a,b) in excellent agreement with previous studies of $OmpA_{171}$ folding into the same lipid environment (Burgess et al., 2008; Danoff and Fleming, 2017). The addition of FkpA to the folding reaction significantly increases the folded fraction of $OmpA_{171}$ to ~70% (Figures 2a and S2a,b), demonstrating that this periplasmic chaperone has a direct beneficial effect on $OmpA_{171}$ folding. Notably, this improved folding in the presence of FkpA is unique; other periplasmic chaperones do not have this effect. SurA, presumably the most utilized periplasmic chaperone in OMP biogenesis (Lazar et al., 1998; Sklar et al., 2007), does not impact $OmpA_{171}$ folding in this assay while Skp maintains the protein almost entirely in the unfolded state over the course of an hour (Figure 2a and S3a) in agreement with previously published results (Schiffrin et al., 2017; Thoma et al., 2015). Beyond changes to the folded population of $OmpA_{171}$, monitoring the unfolded and elusive populations as a function of time provides some insight as well. FkpA maintains a larger fraction of $OmpA_{171}$ in an unfolded state at intermediate timepoints (5–10 min) and decreases the elusive population throughout the folding

reaction (Figure S3a), indicating that FkpA suppresses some lipid-induced aggregation. Together these observations and comparisons to other players in the OMP biogenesis pathway differentiates FkpA and indicates enhancement of OMP folding yields due to the chaperone function of FkpA.

To gain insight into the effect of FkpA on the kinetics of OMP folding, the folding profiles were fit to single exponential functions to obtain observed first-order rate constants (k_{obs}). For $OmpA_{171}$ alone, k_{obs} = 2.0 (±0.7) × 10^{-3} s^{-1} (Figure 2a), which is in good agreement with the previously observed slow component of

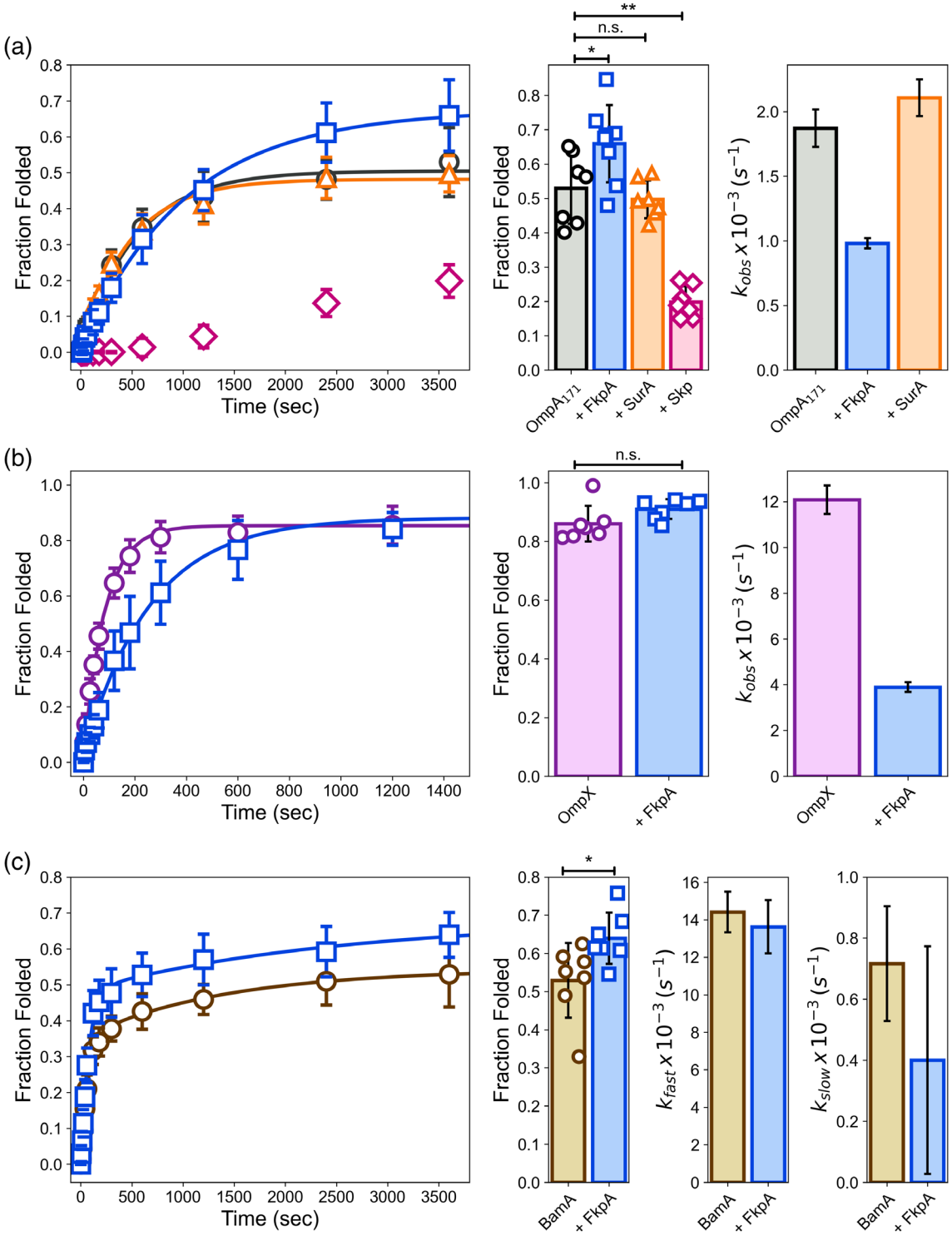

FIGURE 2 Legend on next page.

$OmpA_{171}$ folding (Burgess et al., 2008). Upon adding FkpA to the folding reactions, the observed $OmpA_{171}$ folding rate decreases by a factor of two (k_{obs} = 1.0 [±0.2] × 10^{-3} s^{-1}, Figure 2a). The decrease in $OmpA_{171}$ folding rate in the presence of FkpA indicates that FkpA behaves as a uOMP chaperone and not as a folding catalyst, since folding catalysts (like BamA. e.g., Plummer and Fleming, 2015) increase the rate of uOMP folding. The lack of *cis*-prolines in the primary sequence of $OmpA_{171}$ ensures that the known PPIase activity of FkpA plays no role in improving the folding of $OmpA_{171}$. In fact, *cis*-prolines are generally uncommon among cell envelope proteins (Table S1), suggesting that the chaperone function of FkpA supersedes its PPIase activity in the periplasm. Thus, both the increase in the fraction of $OmpA_{171}$ folded and the decrease in folding rate are attributed to the chaperone function of FkpA.

The presence of FkpA has a comparable effect on the folding of OmpX. Unlike $OmpA_{171}$, OmpX quickly folds with high-efficiency (~85%) into $diC_{11}PC$ LUVs, even in the absence of chaperone (Figure 2b and S3b). As a result, FkpA cannot increase the yield of folded OmpX beyond its already near maximal folding efficiency. However, the presence of FkpA does significantly decrease the OmpX folding rate by a factor of 3 just as FkpA decreases the folding rate of $OmpA_{171}$, indicating a holdase chaperone function where client release limits the overall rate of folding (Figure 2b).

The effect of FkpA on BamA folding differs from its effect on $OmpA_{171}$ or OmpX folding. The addition of FkpA to the folding reaction increases the fraction of folded BamA in the burst phase (i.e., in the 1–2 min of folding) and after 1 h (Figure 2c) but does not significantly alter either rate constant (BamA folding is biphasic). An equivalent decrease in the elusive population of BamA implies that FkpA increases the folded population of BamA by suppressing aggregation (Figure S3c). SV data further corroborates this hypothesis (see Section 2.2). Why FkpA affects the overall rates of $OmpA_{171}$ and OmpX folding but not the overall folding rate of BamA remains unexplained. This discrepancy may suggest that different microscopic rate constants for folding, aggregation, client binding, and client release exist for different uOMPs such that client release from the chaperone is rate-limiting for some uOMPs but not others.

2.2 | FkpA binds and prevents the aggregation of uOMPs

Interpretation of the OMP folding assays assumes chaperone binding, so we verified binding of FkpA to each of the three uOMPs by sedimentation velocity (Figure 3) and photo-crosslinking (Figure 4) experiments. Interactions between two protein binding partners (or lack thereof) may be easily assessed by performing a SV-AUC experiment and comparing the $g(s^*_{20,w})$ distributions of each species alone to the distribution of the mixture. $uOmpA_{171}$ sediments as a single, monomeric species at a concentration of 5 μM in 1 M urea (Figure 3a, Table 1) (Danoff and Fleming, 2011; Tan et al., 2010), while FkpA is dimeric across the experimental concentrations and conditions used in this study (Figure 3a, Table 1, Figures S4 and S5, and see Section "Oligomeric States of FkpA Constructs" in Supplemental Results). For non-interacting systems, the $g(s^*_{20,w})$ distribution is the sum of the distributions of the individual components (shown as a dotted line in Figure 3a). However, the mixture of 30 μM FkpA and 5 μM $uOmpA_{171}$ in 1 M urea produces an experimental $g(s^*_{20,w})$ shifted to larger sedimentation coefficients, indicating binding and the formation of an FkpA: $uOmpA_{171}$ complex (Figure 3a). These results

FIGURE 2 FkpA enhances OMP folding by increasing folded populations and decreasing observed folding rate constants. (a, left) Fraction of $OmpA_{171}$ folded into $diC_{11}PC$ LUVS as a function of time (0–3600 s) in the presence of FkpA (blue squares, $n = 8$), SurA (orange triangles, $n = 7$), or Skp (pink diamonds, $n = 7$) or without any chaperone (black circles, $n = 7$). Lines are single exponential fits to the average data. Folding in the presence of Skp is not fit to an exponential function due to the long lag period. (a, center) Comparison of the fraction of $OmpA_{171}$ folded at 1 h = 3600 s. (a, right) Comparison of the observed rate constants when the average data are fit to single exponential functions. (b, left) Fraction of folded OmpX as a function of time in the presence of FkpA (blue squares, $n = 7$) or without any chaperone (purple circles, $n = 7$). Lines are single exponential fits to the average data. Only the first 1500 s of the reaction are shown to highlight the effect of FkpA early in the folding process. (b, center) Comparison of the fraction of OmpX folded at 1 h = 3600 s. (b, right) Comparison of the observed rate constants when the average data are fit to single exponential functions. (c, left) Fraction of BamA folded as a function of time in the presence of FkpA (blue squares, $n = 7$) or without any chaperone (brown circles, $n = 7$). Lines are single exponential fits to the average data. (c, center left) Comparison of the fraction of BamA folded at 1 h = 3600 s. (c, right) The average BamA folding data fits to a double exponential function, indicating fast and slow rate constants. Both the fast (center right) and slow (far right) rate constants are compared in the presence and absence of FkpA. All error bars represent ±1 standard deviation. For rate constants, the standard deviation was calculated from the covariance matrix obtained by nonlinear least squares fitting of the average data to a single or double exponential function (*$p < 0.05$, **$p < 0.01$, independent *t*-test with unequal variances).

confirm chaperone binding under conditions comparable to those used in the OMP folding assay.

Like $uOmpA_{171}$, uOmpX sediments as a single monomeric species at 5 μM in 1 M urea and clearly binds FkpA as indicated by the rightward shift in the experimental $g(s^*_{20,w})$ distribution of the FkpA and uOmpX mixture (Figure 3b). Unlike the smaller uOMPs, 5 μM uBamA forms aggregated oligomers centered at ~9 Svedberg even in 1 M urea. However, when BamA is diluted into a solution containing FkpA, chaperone binding results in the formation of a complex at ~5.5 Svedberg and fully suppresses the oligomeric state of uBamA (Figure 3C). These SV results confirm chaperone binding under conditions comparable to those used in the OMP folding assay and corroborate the interpretation that FkpA improves BamA folding by preventing aggregation.

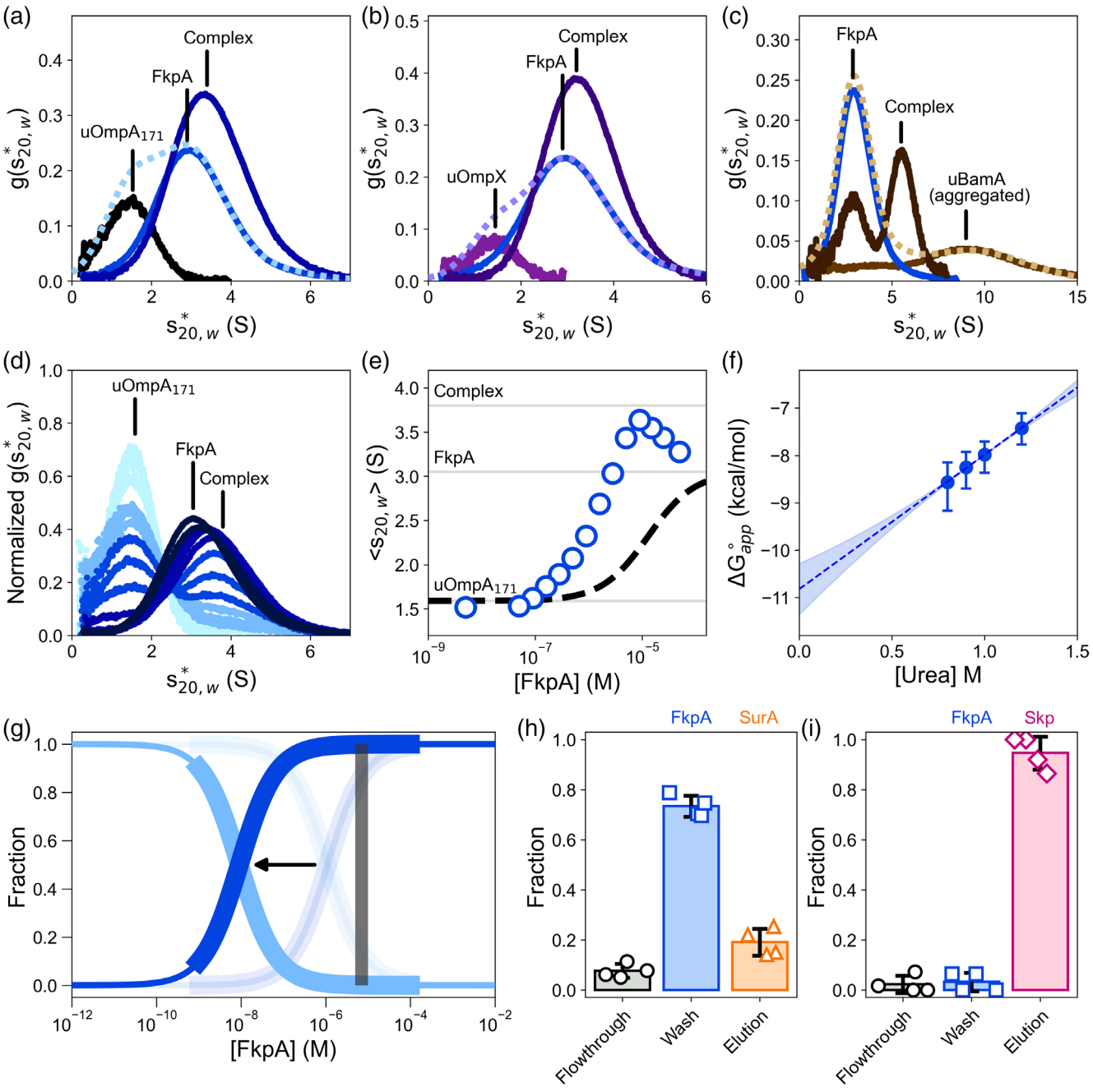

FIGURE 3 Legend on next page.

2.3 | High affinity uOMP binding is highly urea dependent

The chaperone function of FkpA has been demonstrated using a plethora of unfolded or misfolded model clients (Arie et al., 2001; Bothmann and Plückthun, 2000; Hu et al., 2006; Ramm and Plückthun, 2000, 2001; Saul et al., 2004), but the FkpA binding affinity for known, physiologically-relevant uOMP clients is limited. To measure the affinity of FkpA for $uOmpA_{171}$, we titrated 5 μM $uOmpA_{171}$ with increasing FkpA concentrations between 0.01 and 100 μM and followed the interacting system in solution using a series of SV-AUC experiments. Analysis of these titrations revealed the formation of a FkpA:$uOmpA_{171}$ chaperone-client complex. Complex formation is illustrated as both a concentration-dependent shift in the reaction boundary (Figure 3d) and as the change in weight-average $s_{20,w}$ ($<s_{20,w}>$) as a function of FkpA concentration (Figure 3e). The overlaid $g(s^*_{20,w})$ distributions shows the depletion of the unbound $uOmpA_{171}$ population ($s_{20,w}$ = 1.59 Svedberg) and formation of the chaperone-client complex ($s_{20,w}$ = 3.80 Svedberg) as $uOmpA_{171}$ is titrated with FkpA. The reaction boundary and $<s_{20,w}>$ shifts back toward the distribution of unbound FkpA ($s_{20,w}$ = 3.05 Svedberg) due to an increasing population of free FkpA at high concentrations.

To determine the $s_{20,w}$ of the FkpA:$uOmpA_{171}$ complex and the disassociation constant (K_d) for the binding equilibrium, the full titrations were globally fit in SEDANAL (Figure S6) using the model:

$$\mathrm{FkpA} + \mathrm{uOmpA_{171}} \rightleftharpoons \mathrm{FkpA:uOmpA_{171}} \quad (1)$$

Equation (1) assumes a dimeric species of FkpA, which we and others have shown to be the dominant form of FkpA above 1 μM in concentration (see Section "Oligomeric States of FkpA Constructs" in the Supplemental Results) (Arie et al., 2001; Ramm and Plückthun, 2000), and also includes a small fraction of irreversible aggregate that accounts for <1% of the total protein concentration. Sedimentation coefficients for FkpA and $uOmpA_{171}$ were held constant at values obtained from fitting each component alone (Table 1). Globally fitting the titration in 1 M urea results in a K_d = 1.1 (0.6–1.8) μM and a complex $s_{20,w}$ = 3.80 (3.68–3.92) Svedberg. The 95% confidence intervals are reported in parentheses.

Just as chemical denaturants destabilize the native, folded structures of proteins, we speculate that even the low concentrations of urea in our binding titrations modulate the chaperone-client interaction. To investigate the suspected urea dependence of the binding affinity between FkpA and $uOmpA_{171}$, we repeated titrations as a function of the urea concentration. The range of urea concentrations accessible to this type of experiment is narrow as $uOmpA_{171}$ solubility decreases

FIGURE 3 FkpA tightly binds uOMPs and suppresses uOMP aggregation. (a–c) A comparison of $g(s^*_{20,w})$ distributions obtained from SV shows FkpA binding (a) $uOmpA_{171}$, (b) uOmpX, and (c) uBamA. In each experiment, $g(s^*_{20,w})$ distributions of 30 μM FkpA (blue) and 5 μM OMP ($uOmpA_{171}$ = black, uOmpX = purple, uBamA = brown) derive from SV experiments in 1 M urea. Note that while $uOmpA_{171}$ and uOmpA are monomeric and monodisperse in 1 M urea, BamA forms aggregates at ~9 Svedberg. A distribution for non-interacting species was calculated by simple addition of the FkpA and OMP distributions (dotted line, light color). FkpA binding for all three OMPs is observed as a shifted experimental $g(s^*_{20,w})$ distribution (solid line, dark color). In the case of uBamA, aggregation is suppressed when the FkpA:uBamA complex forms. (d and e) FkpA titrating 5 μM $uOmpA_{171}$ is shown as (d) the shift in the reaction boundary and (e) the change in weight-average $s_{20,w}$ ($<s_{20,w}>$) as a function of FkpA concentration. The change in $g(s^*_{20,w})$ distributions and $<s_{20,w}>$ show the depletion of the unbound $uOmpA_{171}$ population ($s_{20,w}$ = 1.59 [1.57–1.61] Svedberg) and formation of the chaperone-client complex ($s_{20,w}$ = 3.80 (3.68–3.92) Svedbergs) as $uOmpA_{171}$ is titrated with FkpA ($s_{20,w}$ = 3.05 [3.04–3.06] Svedberg). $g(s^*_{20,w})$ distributions are colored from light blue to dark blue to correspond with increasing FkpA concentrations. The leftward shift of experimental data away from the line predicted for non-interacting species (black dashed line) in (e) also indicates binding. The reaction boundary and $<s_{20,w}>$ shift back toward that of unbound FkpA due to an increasing population of free FkpA at high FkpA concentrations. (f) Plot of the binding $\triangle G^\circ_{app}$ as a function of urea concentration. A linear fit to the data ($y = 2.8x - 10.8$) allows extrapolation back to 0 M urea where $\triangle G^\circ_{app}$ = −10.8 (−10.3 to −11.3) kcal/mol and K_d = 8 (4–20) nM. Error bars are 95% confidence intervals on the fit calculated using the F-stat module in SEDANAL. (g) The transparent fraction bound and fraction free curves represent the 1 M urea condition. The inflection point shifts leftward by two orders of magnitude in 0 M urea. Fraction of FkpA bound as a function of FkpA concentration, which assumes an obligate dimer at all concentrations, is in blue. Fraction free is light blue. Periplasmic FkpA concentrations are shown in the gray box. In the absence of all other factors, FkpA would be almost entirely bound at its periplasmic concentrations. (h and i) FkpA outcompetes SurA for $uOmpA_{171}$ binding but cannot remove $uOmpA_{171}$ bound to Skp. His-tagged SurA:$uOmpA_{171}$ or Skp:$uOmpA_{171}$complexes were pre-equilibrated on Ni NTA resin (Flowthrough) before washing with untagged FkpA (Wash) and subsequent elution with imidazole (Elution). (h) The greatest fraction of $uOmpA_{171}$ is found in the Wash fractions, indicating that FkpA has a greater affinity for $uOmpA_{171}$ than SurA does. (i) When Skp and FkpA compete for $uOmpA_{171}$ binding, $uOmpA_{171}$ remains bound to Skp and appears almost entirely in the Elution fractions, indicating that Skp has the stronger affinity. Bars are the average of four pulldown experiments, and error bars are ±1 standard deviation.

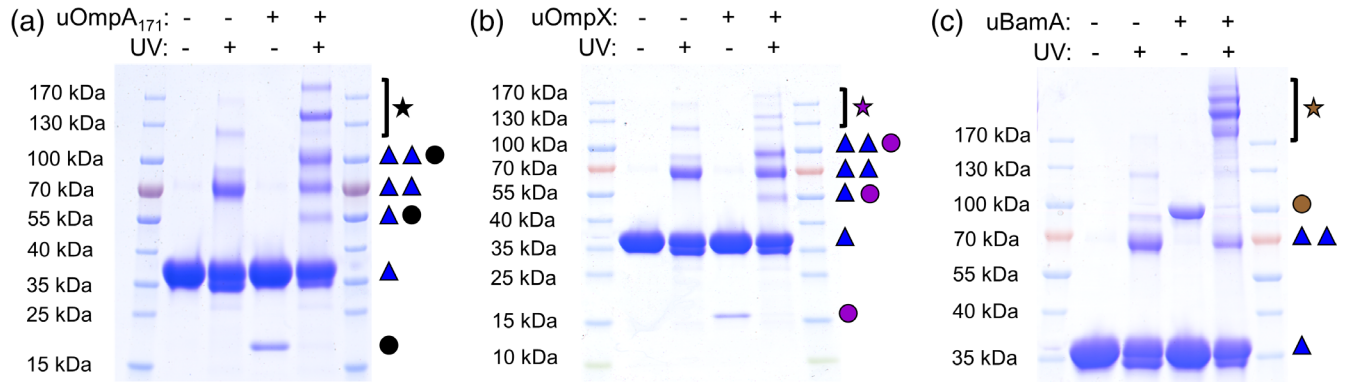

FIGURE 4 FkpA binds and crosslinks to three different uOMPs. The SDS-PAGE readout after photo-crosslinking FkpA variant Y225pAzF with (a) $uOmpA_{171}$ (black circle, ●), (b) uOmpA (purple circle, ●), or (c) uBamA (brown circle, ●) show chaperone:uOMP complex formation. Y225pAzF monomers are labeled with a blue triangle (▲) and uOMPs are labeled with a filled circle. Covalently cross-linked Y225pAzF dimers formed after UV exposure are labeled using two blue triangles (▲▲). Chaperone-client complexes that become photo-crosslinked include Y225pAzF:$uOmpA_{171}$in 1:1 (▲●) and 2:1 (▲▲●) ratios (i.e., a monomer of FkpA and a dimer of FkpA photo-crosslinked to the OMP). Higher order complexes of Y225pAzF alone and Y225pAzF photo-crosslinked to $uOmpA_{171}$ (star) suggest that multiple FkpA dimers can interact with each other and with a uOMP. Both uOmpX and uBamA form equivalent complexes with FkpA, though FkpA:uBamA complexes are too large to discriminate on the gel and are all marked by a star.

TABLE 1 Oligomeric states and sedimentation coefficients of all FkpA constructs.

			$s_{20,w}$ (Svedberg)		
Protein	**Best model**	**RMSD**	**Mon, calc (±SD)**	**Dim, calc (±SD)**	**Exp (95% CI)**
FkpA	Single ideal species,[a] dimer	0.0067	1.82 (±0.15)	2.83 (±0.15)	3.05 (3.04–3.06)
sFkpA	Single ideal species,[a] dimer	0.0063	1.85 (±0.13)	2.84 (±0.14)	3.02 (3.01–3.03)
N-FkpA	Single ideal species, dimer	0.0063	1.12 (±0.10)	1.89 (±0.10)	2.01 (2.00–2.02)
C-FkpA	Single ideal species, monomer	0.0077	1.59 (±0.08)	—	1.62 (1.61–1.63)
$uOmpA_{171}$	Single ideal species, monomer	0.0072	—	—	1.59 (1.57–1.61)

Abbreviations: CI, confidence interval; RMSD, root-mean-square deviation; SD, standard deviation.
[a]Includes irreversible aggregate at <1% of the total protein concentration.

with decreasing urea concentrations (Danoff and Fleming, 2011), and FkpA begins to unfold above 1.5 M urea (Figure S7). Considering these two boundaries, we repeated the titrations in 0.8 M, 0.9 M, and 1.2 M urea. These additional SV-AUC titrations reveal that the binding interaction between FkpA and $uOmpA_{171}$ depends strongly on the urea concentration; in contrast, the sedimentation coefficient of the complex is relatively insensitive to the urea concentration (Table 2, Figures 3f and S8). Analogous to the linear extrapolation method for determining protein stability from denaturation experiments, converting K_d(urea) to $\triangle G^{\circ}_{app}$(urea) allows for linear extrapolation of the binding free energy to 0 M urea (Figure 3F). The apparent K_d decreases to 8 (4–20) nM when extrapolated water. The K_d determined here initially appears more favorable than what is reported for FkpA binding uOmpC in the literature, but after correcting for the urea dependence of the binding constant, both values are in excellent agreement (Ge et al., 2014). Figure 3g illustrates the dramatic effect that even low urea concentrations have on the FkpA:$uOmpA_{171}$ population distribution by comparing fractional binding curves in 0 and 1 M urea.

The steep urea dependence of the FkpA binding affinity (m-value = 2.8 kcal/(mol M)) suggests that an extensive surface area is buried upon client-binding. Using the empirical correlation between urea m-value and the change in accessible surface area (ΔASA) published by Myers et al. (1995) we calculate that FkpA binding to $uOmpA_{171}$ buries approximately 22,000 Å^2 of ASA. The FkpA dimer alone exposes 40,000 Å^2 of ASA while a model of $uOmpA_{171}$ (Marx et al., 2020b) exposes 20,000 Å^2 of ASA. Of the sum total 60,000 Å^2 accessible to the two unbound proteins, about one-third is buried in the binding interface.

TABLE 2 Best fit parameters from global fits of SV-AUC binding titrations.

Protein	[Urea]	Best model	RMSD	Complex $s_{20,w}$ (Svedberg) (95% CI)	K_d (μM) (95% CI)
FkpA	0.8 M	FkpA + $uOmpA_{171}$ ↔ FkpA:$uOmpA_{171}$[a]	0.0078	3.79 (3.69–3.90)	0.4 (0.1–0.8)
	0.9 M	FkpA + $uOmpA_{171}$ ↔ FkpA:$uOmpA_{171}$[a]	0.0081	3.73 (3.63–3.81)	0.7 (0.3–1.2)
	1.0 M	FkpA + $uOmpA_{171}$ ↔ FkpA:$uOmpA_{171}$[a]	0.0071	3.80 (3.68–3.92)	1.1 (0.6–1.8)
	1.2 M	FkpA + $uOmpA_{171}$ ↔ FkpA:$uOmpA_{171}$[a]	0.0072	3.86 (3.64–4.04)	2.9 (1.6–4.9)
sFkpA	1.0 M	sFkpA + $uOmpA_{171}$ ↔ sFkpA:$uOmpA_{171}$[a]	0.0081	4.23 (4.16–4.30)	3.0 (2.6–3.6)
N-FkpA	1.0 M	N-FkpA + $uOmpA_{171}$ ↔ N-FkpA:$uOmpA_{171}$	0.0058	2.73 (2.52–3.03)	44 (28–68)
C-FkpA	1.0 M	Two ideal species	0.0072	—	—

Abbreviations: CI, confidence interval; RMSD, root-mean-square deviation; SV-AUC, sedimentation velocity analytical ultracentrifugation.
[a]Includes irreversible aggregate at <1% of the total protein concentration.

2.4 | The periplasmic chaperone binding hierarchy

FkpA exhibits very favorable client-binding with a disassociation constant in the low nM range when extrapolated to 0 M urea. This binding affinity is stronger than affinities reported for SurA (Bitto and McKay, 2003; Schiffrin et al., 2017; Wu et al., 2011) but weaker than or similar to affinities reported for Skp (Pan et al., 2020; Qu et al., 2007; Wu et al., 2011). To investigate the interactions between periplasmic chaperones in competition for a uOMP client, we performed competition pulldown assays based on the protocol described by Thoma et al. (2015). His-tagged SurA or Skp was premixed with $uOmpA_{171}$ and added to a small batch of Ni NTA resin. After collecting the flowthrough, the original chaperone:$uOmpA_{171}$ complex was washed with untagged FkpA (Wash) before eluting with high imidazole buffer (Elution). If FkpA competes the $uOmpA_{171}$ away from the original chaperone, $uOmpA_{171}$ appears mostly in the Wash fraction. If the original chaperone binds $uOmpA_{171}$ tighter than FkpA does, $uOmpA_{171}$ predominantly appears in the Elution fractions. FkpA does outcompete SurA for $uOmpA_{171}$ binding but cannot pull the $uOmpA_{171}$ away from Skp (Figures 3h,i and S9). These results confirm our direct binding data that FkpA binds uOMPs more favorably than SurA, but Skp shows the most favorable binding of the three chaperones.

2.5 | OMPs crosslink across an extensive inner surface of FkpA

Direct structural characterization of a FkpA:uOMP complex is extremely challenging due to the heterogeneous and dynamic nature of the unfolded OMP. We began to structurally define the binding interface by incorporating the zero-length photo-crosslinker *para*-azido phenylalanine (pAzF) at 24 surface-exposed, non-conserved positions in FkpA using amber suppression (Chin et al., 2002). As had been described previously (Marx et al., 2020b), a uOMP and FkpA pAzF variant were mixed, exposed to ultraviolet (UV) light, and analyzed by SDS-PAGE. Crosslinking efficiency at each position was calculated using the loss of uOMP band intensity after 5 min of UV exposure. Examples of SDS-PAGE readouts from this crosslinking assay using the FkpA pAzF variant Y225pAzF are shown in Figure 4. Y225 is located on the C-domain of FkpA adjacent to the PPIase catalytic site (Saul et al., 2004). FkpA Y225pAzF is a high efficiency crosslinking variant that crosslinks 83.2 ± 1.5% of the original $uOmpA_{171}$ population, shown in Figure 4a as the complete loss of the $uOmpA_{171}$ band intensity (marked by ●) after exposure to UV light. Similarly, 81.0% ± 2.8% of the total uOmpX (Figure 4b) and 81.8% ± 2.2% of the total uBamA (Figure 4c) crosslink to FkpA. It is interesting to note that FkpA crosslinks to the unfolded β-barrel of BamA but not the folded POTRA domains (Figure S10).

Several higher molecular weight bands appear after UV exposure, including bands corresponding to the FkpA dimer (57 kDa, ▲▲), a single FkpA monomer crosslinked to a uOMP (▲●), and an FkpA dimer crosslinked to a uOMP (▲▲●). Larger crosslinked species can also form, suggesting that multiple FkpA dimers may chaperone a single uOMP client. By quantifying the crosslinking efficiencies of all 24 FkpA pAzF variants (Figures 5a and S11) and mapping these crosslinking efficiencies on the crystal structure of FkpA (PDB 1Q6U, Figure 5b), it becomes clear that the chaperone uses an extensive binding interface that spans the inner surfaces of both the N- and C-domains. This large binding interface is consistent with the steep urea dependence of the disassociation constant and suggests that several local interactions contribute to the overall tight binding affinity.

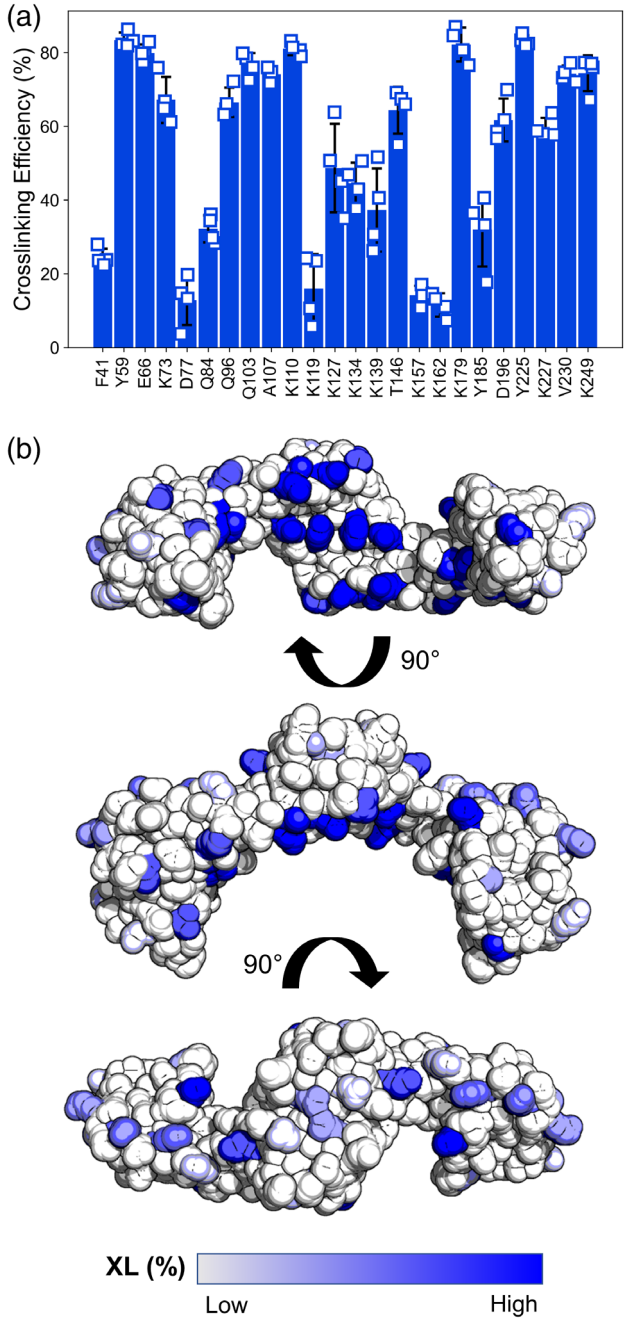

FIGURE 5 FkpA binds uOMPs using an extensive interaction interface. (a) Crosslinking efficiencies calculated using the loss of $uOmpA_{171}$ band intensity for each of the 24 FkpA pAzF variants ($n = 4$, errors bars = ±1 standard deviation). (b) Crosslinking efficiencies shown on the surface of FkpA (PDB 1Q6U). The highest efficiency crosslinking positions are located on the inner surface between the arms of FkpA. High efficiency crosslinking positions are found on both the N- and C-domains.

2.6 | Both structural domains are necessary for tight binding and chaperone function

Previous investigations sought to identify which regions of FkpA contribute to its chaperone function, but conclusions are inconsistent (Arie et al., 2001; Hu et al., 2006; Ramm and Plückthun, 2001; Saul et al., 2004). Because FkpA comprises two distinct structural domains, an N-terminal dimerization domain and a C-terminal PPIase domain, it is tempting to hypothesize that one domain contributes more to binding affinity and chaperone function than the other. However, our photo-crosslinking results suggest that surfaces on both domains contribute to the full binding interface. To further investigate the contributions of the individual domains, we created constructs of the N-terminal domain (N-FkpA) and C-terminal domain (C-FkpA). Both individual domains fold independently, and N-FkpA is dimeric while C-FkpA is monomeric (see Section "Oligomeric States of FkpA Constructs" in the Supplemental Results, Figure S4). When added to $OmpA_{171}$ folding assays, neither domain construct had an effect on the amplitude or rate of $OmpA_{171}$ folding, indicating that neither domain alone is sufficient to recapitulate FkpA chaperone function but that both domains are necessary (Figure S12). The $OmpA_{171}$ folding experiments were also performed in the presence of sFkpA, which has the intrinsically disordered tails at the N- and C-termini of FkpA removed. Previous studies suggest that these IDRs have no functional importance in vitro (Hu et al., 2006; Saul et al., 2004) or in vivo (Ge et al., 2014), and while results from $OmpA_{171}$ folding in the presence of sFkpA are not significantly different from $OmpA_{171}$ folding alone (Figure S10), sFkpA does follow the same trends as full-length FkpA to slightly increase $OmpA_{171}$ folding efficiency and slow the $OmpA_{171}$ folding rate. Therefore, we cannot draw any conclusions about the functional importance of the IDRs from these results.

The $OmpA_{171}$ folding assays revealed that neither FkpA domain alone demonstrates the full chaperone activity, so we evaluated their contributions to $uOmpA_{171}$ binding using SV-AUC titrations. Both sFkpA and N-FkpA appear to bind $uOmpA_{171}$ based on the comparison of calculated and experimental $g(s^*_{20,w})$ distributions (Figure 6a,b). The fit binding constants and sedimentation coefficients are reported in Table 2. sFkpA binds $OmpA_{171}$ with a $K_d = 3.0$ (2.6–3.6) μM in 1 M urea, indicating that the intrinsically disordered tails have no effect on binding affinity when compared to full-length FkpA under the same experimental conditions. N-FkpA weakly binds with a K_d of 44 (28–68) μM. However, calculated and experimental $g(s^*_{20,w})$ distributions overlay for C-FkpA binding to $uOmpA_{171}$, indicating no interaction (Figure 6c). Indeed, this titration was best fit by a two ideal species model, and therefore, any affinity between C-FkpA and $uOmpA_{171}$, if it exists, is too weak to be measured under these experimental conditions. Together these results indicate that while N-FkpA has some

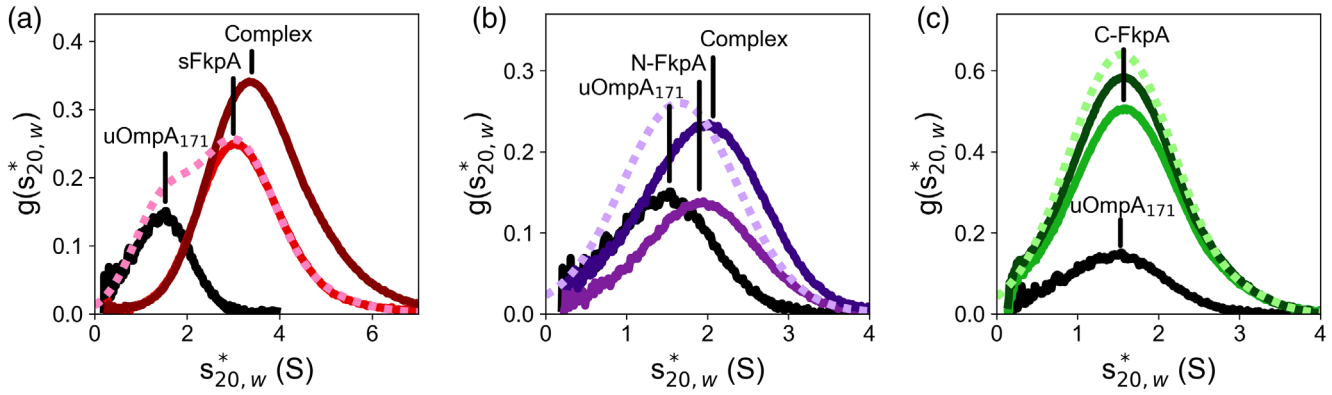

FIGURE 6 Shifted $g(s^*_{20,w})$ distributions when titrating $uOmpA_{171}$ with sFkpA and N-FkpA indicate binding. Distributions of 5 μM $uOmpA_{171}$ (black) and (a) 30 μM of sFkpA (red), (b) 50 μM of N-FkpA (purple), or (c) 50 μM of C-FkpA (green) were added to calculate the distribution for non-interacting species (dashed lines, light color). Experimental reaction boundaries (solid lines, dark color) shifted to the right indicate that sFkpA, and N-FkpA bind $uOmpA_{171}$ at these concentrations. C-FkpA does not.

affinity for $uOmpA_{171}$, both domains are required to achieve the most favorable binding.

3 | DISCUSSION

OMP biogenesis requires a network of chaperones to keep uOMPs in an unfolded but folding-competent state in the aqueous environment of the periplasm. SurA, Skp, DegP, Spy, and FkpA have all been implicated in this periplasmic chaperone network (He et al., 2021; Missiakas et al., 1996), but the function of FkpA with respect to the OMP biogenesis pathway has been under-investigated as compared to other chaperones (Figure 7). Here we show that FkpA binding and chaperoning of uOMPs affects their folding trajectory, which to our knowledge is the first study to demonstrate a direct enhancement of OMP folding by FkpA. Generally, FkpA can increase the folding yield of OMPs into $diC_{11}PC$ LUVs after 1 h and decrease the overall rate of OMP folding by (1) suppressing aggregation as is the case for BamA, (2) introducing a rate-limiting chaperone release step as observed for OmpX, or (3) a combination of both effects, which best explains the $OmpA_{171}$ folding results. The fact that FkpA does not impact the folding rate of BamA suggests that chaperone release is not a rate-limiting step for this OMP and implies that there may exist different kinetic competitions between aggregation, folding, client binding, and client release in the biogenesis of different OMPs.

Despite the known redundancy encoded in the essentiality of the periplasmic chaperones, FkpA has a markedly different impact on $OmpA_{171}$ folding as compared to the chaperones SurA or Skp. In contrast to FkpA, the addition of SurA to the folding reaction had no effect on $OmpA_{171}$ folding, a finding that recapitulates previously published experiments investigating the folding of $OmpA_{171}$ and PagP (McMorran et al., 2013; Schiffrin et al., 2017). This result in itself is somewhat surprising as SurA is thought to be the most important periplasmic chaperone in the OMP biogenesis pathway based on its phenotypic growth defect and the decrease in folded OMP levels upon SurA deletion (Lazar et al., 1998; Sklar et al., 2007). However, the function of SurA is thought to be linked to the BAM complex as evidenced by genetic and structural interactions between SurA and BAM (Schiffrin et al., 2022; Sklar et al., 2007). Additionally, recent literature supports a model where SurA binds extended conformations of uOMPs using localized and regulated binding regions (Calabrese et al., 2020; Jia et al., 2020; Marx et al., 2020a, 2020b; Soltes et al., 2016), leading to a weaker binding in the high nM to low μM range (Bitto and McKay, 2003; Schiffrin et al., 2017; Wu et al., 2011). Quick client binding and release combined with a proposed interaction with and rate enhancement of BAM may explain why SurA can improve OMP folding in the presence of BAM but has little to no intrinsic ability to improve OMP folding efficiency by itself (Hagan et al., 2010; Wu et al., 2021). Also in contrast to FkpA, the trimeric chaperone Skp keeps almost the entire population of $OmpA_{171}$ in the unfolded state for the duration of the folding reaction, with only a small fraction of $OmpA_{171}$ folding after a significant lag period. The effect of Skp is explained by its high affinity for uOMPs. Three monomers form a claw-like trimer with an internal cavity that sequesters a single uOMP chain, blocking aggregation with other chains (Walton et al., 2009; Walton and Sousa, 2004; Zaccai et al., 2016). In this binding mechanism, a flexible Skp accommodates dynamic uOMPs through many non-specific interactions (Burmann

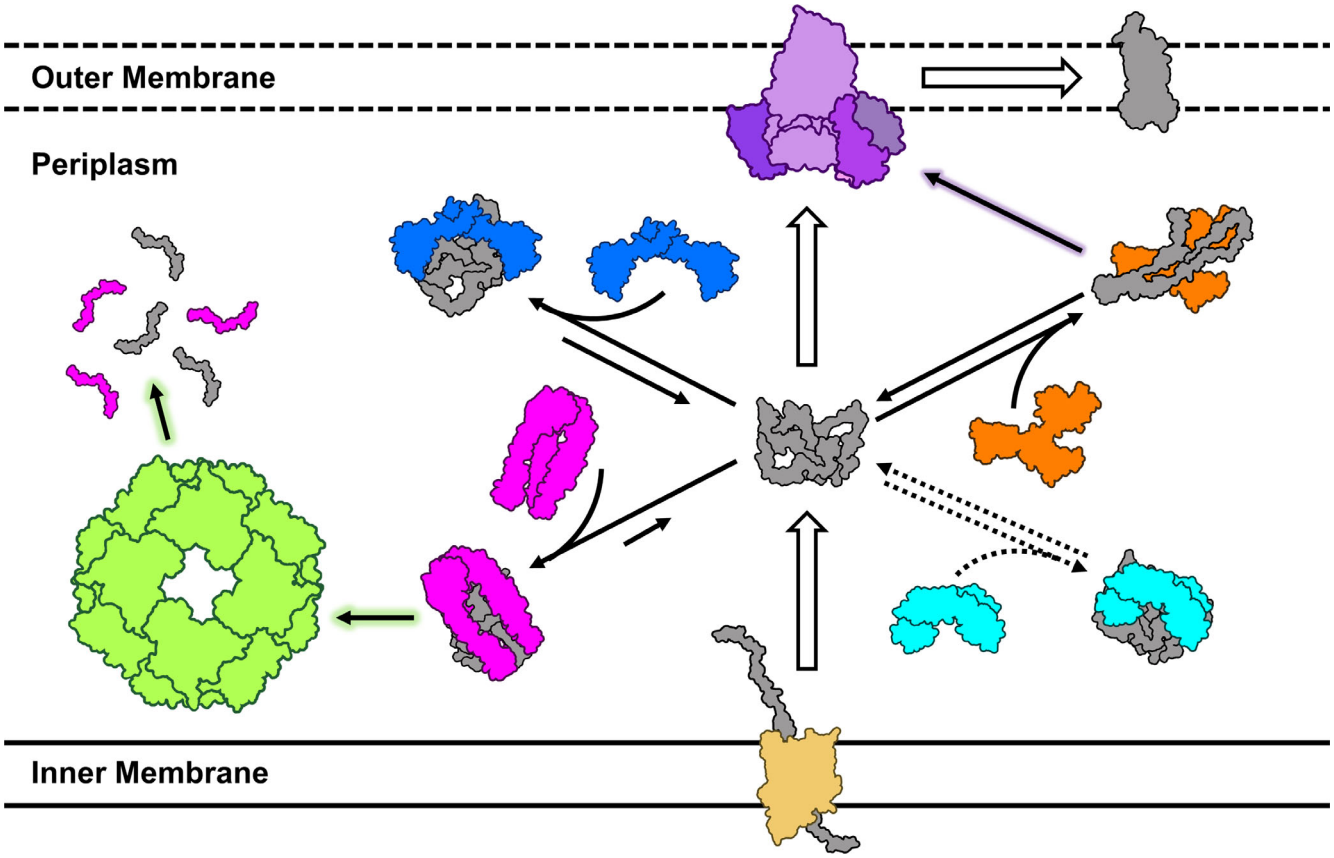

FIGURE 7 Schematic of the OMP biogenesis periplasmic chaperone network. As uOMPs are translocated into the periplasm, a network of periplasmic chaperones maintains uOMPs in an unfolded, but folding competent state before they fold into the membrane (white arrows) aided by the catalytic BAM complex (purple). FkpA (blue), Skp (pink), Spy (aqua), DegP (green), and SurA (orange) are members of this periplasmic network. Tight binders like Skp and FkpA favor the chaperone:uOMP complex to act as holdases that prevent uOMP aggregation. The tightly bound Skp complex can also be degraded by the protease DegP (green arrow). Spy moonlights as an uOMP chaperone that binds some uOMPs with weak affinity (dotted arrows). SurA weakly binds uOMPs but contributes to the uOMP folding process by extending the unfolded polypeptides and handing off clients to the BAM complex (purple arrow).

et al., 2013) that contribute to an overall affinity in the high pM to low nM range (Pan et al., 2020; Qu et al., 2007; Wu et al., 2011). Because Skp binds uOMPs so tightly, they remain bound to the chaperone pool instead of folding into the lipid vesicles.

The fact that FkpA can improves uOMP folding yields over the course of an hour distinguishes FkpA from the other periplasmic chaperones, but FkpA does not behave as a folding catalyst like the BAM complex (Hagan et al., 2010; Plummer and Fleming, 2015; Schiffrin et al., 2017). Unlike a folding catalyst, FkpA can decrease the rate of folding, suggesting that client release from the chaperone becomes the rate-limiting step for some uOMPs. Moreover, it is clear that the effect of FkpA on OMP folding originates from its chaperone activity and not its PPIase activity. While FkpA is known to efficiently catalyze peptidyl-prolyl *cis*/*trans* isomerization in a range of peptide and full-length protein substrates (Arie et al., 2001; Ramm and Plückthun, 2000, 2001), the sequence of $OmpA_{171}$ in particular does not include any *cis* prolines (Table S4). In fact, *cis* prolines are rare among both outer membrane and periplasmic proteins in general (Table S4), suggesting that the PPIase domain has been evolutionarily repurposed in periplasmic chaperones.

Attributing the effect of FkpA on OMP folding to a holdase activity is the simplest explanation. The strength of the interaction between FkpA and a uOMP may be optimized to promote folding and prevent aggregation. However, without increased molecular resolution, we cannot rule out the possibility that FkpA actively assists in uOMP folding, perhaps by stabilizing secondary structures in the unfolded ensemble before membrane insertion. Further work to elucidate the kinetics of FkpA client-binding and release and the structural features of an FkpA:uOMP complex are needed to fully explain the effect of FkpA on OMP folding.

Interpretation of the folding assays assumes chaperone binding, so we verify that FkpA binds $uOmpA_{171}$,

uOmpX, and uBamA with SV and crosslinking assays. Furthermore, we find that FkpA ($K_d \sim 10$ nM) binds to uOMPs with an affinity that is intermediate between that of SurA ($K_d \sim 1$ μM) and Skp ($K_d \sim 1$ nM). Therefore, in a direct competition of periplasmic chaperones, this implies that Skp ≥ FkpA > SurA in terms of individual binding affinity. One could argue that stable binding in the low nanomolar range is inconsistent with a chaperone function. However, as long as the rate of client release is fast enough, even small disassociation constants can be consistent with uOMP flux across the periplasm as has been previously shown (Costello et al., 2016). Even a disassociation rate on the order of seconds (Ge et al., 2014) may be fast enough for facilitated diffusion of uOMPs without requiring additional factors to stimulate client release. However, we recognize that the periplasm is a complex environment where factors such as membrane charges, interactions with other periplasmic chaperones, the presence of the BAM complex, or self-regulation encoded in the conformational heterogeneity of FkpA may trigger client release as well. It is also possible that FkpA:uOMP complexes may be fully degraded by DegP as has recently been shown for tightly bound Skp–uOMP complexes (Figure 7) (Combs and Silhavy, 2022).

Previous work has suggested that the chaperone function of FkpA is localized to either the N-terminal dimerization (Arie et al., 2001; Saul et al., 2004) or the C-terminal PPIase domain (Hu et al., 2006; Ramm and Plückthun, 2001), but we find that neither domain alone exhibits chaperone function or high affinity uOMP binding. Some binding of $uOmpA_{171}$ to N-FkpA was observed even though it was 10-fold weaker than the binding of the full-length protein, which may explain why N-FkpA prevented protein aggregation in some *in vitro* assays but was unable to rescue periplasmic stress when introduced into a *ΔfkpA ΔdegP* deletion strain (Saul et al., 2004). Results from the domain deletion constructs indicate that both domains in the full-length protein are required for full chaperone activity and tight client-binding. This is also consistent with the pAzF crosslinking assays, which indicate that the binding interface on FkpA spans the N- and C-domains with high efficiency crosslinking residues localized to regions on the inner surfaces of both. By bringing the two PPIase domains in close proximity via dimerization of the N-domain, FkpA increases the available binding surface and locally increases the number of interactions that contribute to the overall binding affinity. It should be noted that only the chaperone function of FkpA is dependent on both structural domains as the C-domain alone catalyzes peptidyl-prolyl isomerization reactions (Arie et al., 2001; Ramm and Plückthun, 2001). Due to the extensive binding interface on the chaperone, the FkpA:uOMP interaction is highly sensitive to the concentration of denaturant in solution. From the urea dependence of the binding constant, we estimate that approximately 22,000 Å^2 of accessible surface area is buried when $uOmpA_{171}$ binds FkpA (which is roughly equivalent to the ΔASA upon folding of α-chymotrypsin) (Myers et al., 1995). Parameters like ΔASA and $s_{20,w}$ of the complex obtained from the SV-AUC experiments are useful to constrain possible structures of an FkpA:uOMP complex.

The distinct effect of FkpA on OMP folding requires the full-length, dimeric protein and suggests that FkpA client binding and release are optimized to suppress aggregation but allow folding in a way that SurA and Skp alone cannot. The intermediate-to-tight binding mediated by a large interaction surface on the chaperone contributes to this general but potent chaperone strategy. In the context of the periplasmic chaperone network, the presence of FkpA ensures a robust response to stress, including environmental stresses encountered by virulent strains, by complementing the other unique roles of Skp and SurA (Figure 7, green and purple arrows). Continued work toward obtaining structural information on a FkpA:uOMP complex, exploring the conformation heterogeneity of FkpA, and quantifying the rate of FkpA client binding and release will help elucidate the full mechanism of FkpA chaperone function. As FkpA chaperones many unfolded, partially folded, or misfolded proteins other than its known OMP clients (OmpC (Ge et al., 2014) and now $OmpA_{171}$, OmpX, and BamA), continued discovery of additional FkpA clients will help elucidate how an effective ATP-independent chaperone like FkpA balances the trade-off between specificity and promiscuity and functions to manage OMP biogenesis under periplasmic stress conditions.

4 | MATERIALS AND METHODS

4.1 | Expression and purification of proteins

Cytoplasmic expression and purification of soluble chaperones SurA, Skp, and all FkpA constructs is detailed in Appendix S1. Purification of OMPs from inclusion bodies can also be found in Appendix S1.

4.2 | Outer membrane protein folding assays

The preparation of $diC_{11}PC$ LUVs and execution of OMP folding assays were modified from those conducted in Burgess et al. (2008) and Danoff and Fleming (2017). For

a full description of these experiments, refer to Appendix S1.

4.3 | Sedimentation velocity analytical ultracentrifugation binding titrations and analysis

The oligomeric states of each FkpA construct and their binding to $uOmpA_{171}$, uOmpX, and uBamA were determined using sedimentation velocity analytical ultracentrifugation (SV-AUC). Samples of each FkpA construct (FkpA, sFkpA, N-FkpA, and C-FkpA) were prepared at a series of concentrations between 1 and 150 μM in phosphate buffer (20 mM sodium phosphate, pH 8) supplemented with 1 M urea. All concentrations are the total monomer concentrations. A concentration series of FkpA in phosphate buffer was also prepared to verify that 1 M urea has no effect on the oligomerization of FkpA. To first verify binding to each of the three uOMPs, 5 μM uOMP was mixed with 30 μM FkpA, and formation of the chaperone:uOMP complex was determined by comparing $g(s^*_{20,w})$ distributions. A binding constant for FkpA binding a uOMP was determined by titrating 5 μM $uOmpA_{171}$ with each FkpA construct using 1 nM to 150 μM of the chaperone. FkpA titrations were repeated in 0.8 M, 0.9 M and 1.2 M urea. The sedimentation of 5 μM $uOmpA_{171}$ has been previously shown to be monomeric and monodisperse in 1 M urea (Danoff and Fleming, 2011; Tan et al., 2010), which was verified by spinning 5 μM $OmpA_{171}$ in phosphate buffer plus 1 M urea in triplicate. uOmpX is also monomeric and monodisperse at 5 μM, but uBamA forms oligomers centered at ~9 Svedberg.

All SV-AUC experiments were performed using a Beckman XL-A ultracentrifuge (Beckman Coulter) and cells with 1.2 mm double-sector epoxy centerpieces and sapphire windows. Each sample was spun at 20°C using a 4-hole, An-Ti60 rotor and speed of 50,000 rpm for up to 200 scans. Radial scans were acquired with 0.003 cm radial steps in continuous mode no delay between scans. A wavelength of 230, 250, or 280 nm was chosen for each experiment such that the sample absorbance was always in the linear optical range of 0.1–1.0 absorbance units. Extinction coefficients (Table S3) at 230 nm and 250 nm were obtained from the slope of calibration curves created with a series of known protein concentrations (data not shown). Prior to starting each run, the rotor was temperature equilibrated in the instrument for at least 60 min.

All SV-AUC data was analyzed using dc/dt+ (Philo, 2006) and SEDANAL (Stafford and Sherwood, 2004). Sedimentation coefficient distributions ($g(s^*_{20,w})$ distributions) were created using dc/dt+ and were corrected using the appropriate densities (ρ), viscosities (η), and partial specific volumes ($\bar{\nu}$) for each buffer and protein construct calculated using SEDNTERP (Table S4) (Laue et al., 1992). Full FkpA concentration series were first globally fit in SEDANAL to determine the oligomeric state of each construct alone. The best-fit models and statistics describing these fits can be found in Table 1. To obtain the best fit, a small (<1%) fraction of irreversible FkpA aggregate was included in the model when fitting FkpA and sFkpA concentration series.

Binding titrations were globally fit in SEDANAL to determine disassociation constants (K_d) and the sedimentation coefficients of the chaperone-$uOmpA_{171}$ complex. FkpA and sFkpA titrations were fit to a FkpA + $uOmpA_{171}$ ↔ FkpA:$uOmpA_{171}$ binding model including the irreversible FkpA aggregate at <1% of the total protein concentration. The N-FkpA titration could also be fit to the simple N-FkpA + $uOmpA_{171}$ ↔ N-FkpA:$uOmpA_{171}$ model, but the C-FkpA titration was best described by two ideal species that do not interact and thus no binding could be observed. The sedimentation coefficients of $uOmpA_{171}$and each FkpA construct was held fixed at its previously determined value when fitting the corresponding binding titration. For all global fits, goodness-of-fit was assessed by minimization of residuals reflected in the root-mean-square deviation (RMSD), by the randomness of the residuals, and narrowness of the 95% confidence interval on fitted parameters. Confidence intervals were determined using the F-statistic module in SEDANAL (Table 2). Sedimentation coefficients from SEDANAL fits were corrected to 20°C in water using Equation (2).

$$s_{20,w} = \frac{(1-\bar{\nu}\rho)_{20,w}\eta_{exp}}{(1-\bar{\nu}\rho)_{exp}\eta_{20,w}} s_{exp} \quad (2)$$

Dissociation constants from globally fitting binding titrations at the four urea concentrations were converted to $\triangle G^\circ_{app}$. Plots of $\triangle G^\circ_{app}$ versus urea concentration were linearly extrapolated to determine the binding constant in 0 M urea. The slope of the line corresponds to the *m*-value, which was used to estimate the ΔASA based on the relationship between the two parameters published by Myers et al. (1995). The ASAs of FkpA and $uOmpA_{171}$ individually were calculated using the FreeSASA module in Python (Mitternacht, 2016) on PDB structures of the FkpA dimer (PDB 1Q6U) and a model of unfolded $OmpA_{171}$ published in Marx et al. (2020b).

4.4 | Chaperone competition pulldown assays

To explore how FkpA binds $uOmpA_{171}$ in the context of other periplasmic chaperones, we designed a

chaperone competition experiment based on a previously published assay (Thoma et al., 2015). Specifically, we investigated whether FkpA can outcompete SurA or Skp for uOMP binding. To compare SurA and FkpA, 20 μM His-tagged SurA was mixed with 5 μM $uOmpA_{171}$ in phosphate buffer containing 1 M urea. A total volume of 1 mL was loaded onto 500 μL of Ni-NTA sepharose high performance resin in a 1.5 mL Eppendorf tube and allowed to equilibrate for 5 min. The flowthrough was collected by centrifugation for 5 min at 14,000 rpm in an Eppendorf tabletop centrifuge. All subsequent wash and elution steps were also equilibrated on the resin for 5 min and collected by centrifugation. Then 1 mL of 40 μM untagged FkpA in phosphate buffer containing 1 M urea was added to the resin to compete with SurA in binding $uOmpA_{171}$ (FkpA Wash). A second wash using 1 mL of Buffer A followed the FkpA Wash. Protein remaining bound to the column was eluted by adding 2× 1 mL of Buffer B to the column. To compare FkpA and Skp, 30 μM His-tagged Skp was mixed with 5 μM $uOmpA_{171}$ in phosphate buffer containing 200 mM NaCl and 1 M urea. The pulldown assay was performed using the above protocol except that Skp bound to the column was eluted by adding 4× 1 mL of Buffer B to the column followed by a single elution with 1 mL of Buffer C.

SDS-PAGE samples were prepared by combining 15 μL of each flowthrough, wash, or elution with 5 μL of 4 X SDS Loading Buffer and heating at 95°C for 5 min. Samples were run on 4–20% gradient precast gels (Mini-PROTEAN TGX; Bio-Rad) run at a constant voltage of 200 V for 35 min at room temperature. The intensity of the $uOmpA_{171}$ band in each lane was determined using densitometry analysis in ImageJ. The intensities in all wash steps and all elution steps were added to the cumulative values reported in Figure 3d,e.

4.5 | Photo-crosslinking assays

Samples of 50 μM of each FkpA pAzF variant alone and 50 μM of the FkpA pAzF variant mixed with 5 μM uOMP ($uOmpA_{171}$, uOmpX, or uBamA) in phosphate buffer plus 1 M urea were prepared in a total volume of 40 μL then split into two aliquots of 15 μL each. One of the two aliquots (UV-treated sample) was then irradiated with UV light (wavelength, $\lambda = 254$ nm) for 5 min using a Spectroline MiniMax UV Lamp (11-992-662; Fisher) to cross-link the species in solution. Each control (no UV exposure) and UV-treated aliquot was denatured by addition of 5 μL of 4 X SDS Loading Buffer and heating at 95 °C for 5 min. Samples were subjected to SDS-PAGE using a 4–20% gradient precast gel (Mini-PROTEAN TGX; Bio-Rad) run at a constant voltage of 200 V for 35 min at room temperature. Using ImageJ, densitometry analysis on the uOMP bands in the control (I_{-UV}) and UV-treated (I_{+UV}) conditions was utilized to quantitate crosslinking efficiency (XL Efficiency) according to Equation (3). Crosslinking efficiency values were corrected for the amount of uOMP lost (~11%) when mixed with wild-type, full-length FkpA (not containing pAzF) and subject to UV irradiation (correction factor = CF). A representative SDS-PAGE gel for photo-crosslinking between each FkpA pAzF variant and $uOmpA_{171}$ is shown in Figure S11.

$$\text{XL Efficiency}\,(\%) = \frac{I_{-UV} - I_{+UV}}{I_{-UV}} * 100 - \text{CF} \qquad (3)$$

All other materials and methods can be found in Appendix S1.

AUTHOR CONTRIBUTIONS

Taylor Devlin: Conceptualization (equal); data curation (lead); formal analysis (lead); investigation (lead); methodology (equal); visualization (lead); writing – original draft (lead); writing – review and editing (equal). **Dagan C Marx:** Conceptualization (equal); data curation (supporting); formal analysis (supporting); investigation (equal); methodology (supporting); supervision (supporting); writing – review and editing (supporting). **Michaela A Roskopf:** Data curation (supporting); formal analysis (supporting); investigation (supporting); methodology (supporting); writing – review and editing (supporting). **Quenton R Bubb:** Data curation (supporting); formal analysis (supporting); investigation (supporting); methodology (supporting); writing – review and editing (supporting). **Ashlee M Plummer:** Conceptualization (supporting); data curation (supporting); formal analysis (supporting); investigation (supporting); methodology (supporting); supervision (supporting); writing – review and editing (supporting). **Karen G Fleming:** Conceptualization (lead); data curation (supporting); formal analysis (supporting); funding acquisition (lead); investigation (supporting); methodology (supporting); project administration (lead); resources (lead); supervision (lead); writing – review and editing (equal).

ACKNOWLEDGMENTS

We thank the Center for Molecular Biophysics for providing facilities and resources. The authors thank lab members for helpful discussions. This work was funded by National Science Foundation (NSF) grants MCB 1931211 (Karen G. Fleming). Taylor Devlin, Dagan C. Marx, and Ashlee M. Plummer were supported by National Institutes of Health (NIH) training grant T32-GM008403.

Ashlee M. Plummer was supported by NSF Grant DGE 1232825.

CONFLICT OF INTEREST STATEMENT

We have no conflicts of interest to declare.

DATA AVAILABILITY STATEMENT

The data that support the findings of this study are available from the corresponding author upon reasonable request.

ORCID

Karen G. Fleming https://orcid.org/0000-0001-5417-8830

REFERENCES

Arie J-P, Sassoon N, Betton J-M. Chaperone function of FkpA, a heat shock prolyl isomerase, in the periplasm of *Escherichia coli*. Mol Microbiol. 2001;39:199–210.

Bitto E, McKay DB. The periplasmic molecular chaperone protein SurA binds a peptide motif that is characteristic of integral outer membrane proteins. J Biol Chem. 2003;278:49316–22.

Bothmann H, Plückthun A. The periplasmic *Escherichia coli* peptidylprolyl *cis,trans*-isomerase FkpA: I. Increased functional expression of antibody fragments with and without *cis*-prolines. J Biol Chem. 2000;275:17100–5.

Burgess NK, Dao TP, Stanley AM, Fleming KG. β-Barrel proteins that reside in the *Escherichia coli* outer membrane in vivo demonstrate varied folding behavior in vitro. J Biol Chem. 2008;283:26748–58.

Burmann BM, Wang C, Hiller S. Conformation and dynamics of the periplasmic membrane-protein-chaperone complexes OmpX-Skp and tOmpA-Skp. Nat Struct Mol Biol. 2013;20:1265–72.

Calabrese AN, Schiffrin B, Watson M, Karamanos TK, Walko M, Humes JR, et al. Inter-domain dynamics in the chaperone SurA and multi-site binding to its outer membrane protein clients. Nat Commun. 2020;11:1–16.

Chin JW, Santoro SW, Martin AB, King DS, Wang L, Schultz PG. Addition of *p*-azido-L-phenylalanine to the genetic code of *Escherichia coli*. J Am Chem Soc. 2002;124:9026–7.

Combs AN, Silhavy TJ. The sacrificial adaptor protein Skp functions to remove stalled substrates from the β-barrel assembly machine. Proc Natl Acad Sci USA. 2022;119:e2114997119.

Costello SM, Plummer AM, Fleming PJ, Fleming KG. Dynamic periplasmic chaperone reservoir facilitates biogenesis of outer membrane proteins. Proc Natl Acad Sci U S A. 2016;113:4794–800.

Cumby N, Reimer K, Mengin-Lecreulx D, Davidson AR, Maxwell KL. The phage tail tape measure protein, an inner membrane protein and a periplasmic chaperone play connected roles in the genome injection process of E. coli phage HK97. Mol Microbiol. 2015;96:437–47.

Danese PN, Silhavy TJ. The σ^E and the Cpx signal transduction systems control the synthesis of periplasmic protein-folding enzymes in *Escherichia coli*. Genes Dev. 1997;11:1183–93.

Danoff EJ, Fleming KG. The soluble, periplasmic domain of OmpA folds as an independent unit and displays chaperone activity by reducing the self-association propensity of the unfolded OmpA transmembrane β-barrel. Biophys Chem. 2011;159:194–204.

Danoff EJ, Fleming KG. Aqueous, unfolded OmpA forms amyloid-like fibrils upon self-association. PLoS One. 2015;10:1–11.

Danoff EJ, Fleming KG. Novel kinetic intermediates populated along the folding pathway of the transmembrane β-barrel OmpA. Biochemistry. 2017;56:47–60.

DeLano WL. The PyMOL molecular graphics system (2.5.0). Schrodinger, LLC; 2015.

Dwyer RS, Malinverni JC, Boyd D, Beckwith J, Silhavy TJ. Folding LacZ in the periplasm of *Escherichia coli*. J Bacteriol. 2014;196:3343–50.

Ge X, Lyu ZX, Liu Y, Wang R, Zhao XS, Fu X, et al. Identification of FkpA as a key quality control factor for the biogenesis of outer membrane proteins under heat shock conditions. J Bacteriol. 2014;196:672–80.

Gunnarsen KS, Kristinsson SG, Justesen S, Frigstad T, Buus S, Bogen B, et al. Chaperone-assisted thermostability engineering of a soluble T cell receptor using phage display. Sci Rep. 2013;3.

Gunnarsen KS, Lunde E, Kristiansen PE, Bogen B, Sandlie I, Løset GÅ. Periplasmic expression of soluble single chain T cell receptors is rescued by the chaperone FkpA. BMC Biotechnol. 2010;10:8.

Hagan CL, Kim S, Kahne D. Reconstitution of outer membrane protein assembly from purified components. Science. 2010;328:890–2.

He W, Yu G, Li T, Bai L, Yang Y, Xue Z, et al. Chaperone spy protects outer membrane proteins from folding stress via dynamic complex formation. MBio. 2021;12:e0213021.

Holdbrook DA, Burmann BM, Huber RG, Petoukhov MV, Svergun DI, Hiller S, et al. A spring-loaded mechanism governs the clamp-like dynamics of the Skp chaperone. Structure. 2017;25:1079–88.

Hu K, Galius V, Pervushin K. Structural plasticity of peptidyl-prolyl isomerase sFkpA is a key to its chaperone function as revealed by solution NMR. Biochemistry. 2006;45:11983–91.

Hu K, Plückthun A, Pervushin K. Backbone Hn, N, Cα, C′ and Cβ chemical shift assignments and secondary structure of FkpA, a 245-residue peptidyl-prolyl cis/trans isomerase with chaperone activity. J Biomol NMR. 2004;28:405–6.

Humes JR, Schiffrin B, Calabrese AN, Higgins AJ, Westhead DR, Brockwell DJ, et al. The role of SurA PPIase domains in preventing aggregation of the outer-membrane proteins tOmpA and OmpT. J Mol Biol. 2019;431:1267–83.

Jia M, Wu B, Yang Z, Chen C, Zhao M, Hou X, et al. Conformational dynamics of the periplasmic chaperone SurA. Biochemistry. 2020;59:3235–46.

Kleinschmidt JH, Den Blaauwen T, Driessen AJM, Tamm LK. Outer membrane protein A of *Escherichia coli* inserts and folds into lipid bilayers by a concerted mechanism. Biochemistry. 1999;38:5006–16.

Kleinschmidt JH, Tamm LK. Folding intermediates of a β-barrel membrane protein. Kinetic evidence for a multi-step membrane insertion mechanism. Biochemistry. 1996;35:12993–3000.

Kleinschmidt JH, Tamm LK. Secondary and tertiary structure formation of the β-barrel membrane protein OmpA is synchronized and depends on membrane thickness. J Mol Biol. 2002;324:319–30.

Laue TM, Shah BD, Ridgeway TM. Pelletier SL computer-aided interpretation of analytical sedimentation data for proteins. In:

Harding S, Rowe A, Hoarton J, editors. Analytical ultracentrifugation in biochemistry and polymer science. Cambridge, UK: Royal Society of Chemistry; 1992. p. 90–125.

Lazar SW, Almirón M, Tormo A, Kolter R. Role of the *Escherichia coli* SurA protein in stationary-phase survival. J Bacteriol. 1998; 180:5704–11.

Marx DC, Leblanc MJ, Plummer AM, Krueger S, Fleming KG. Domain interactions determine the conformational ensemble of the periplasmic chaperone SurA. Protein Sci. 2020a;10:2043–2053.

Marx DC, Plummer AM, Faustino AM, Devlin T, Roskopf MA, Leblanc MJ, et al. SurA is a cryptically grooved chaperone that expands unfolded outer membrane proteins. Proc Natl Acad Sci U S A. 2020b;117:28026–35.

Mas G, Burmann BM, Sharpe T, Claudi B, Bumann D, Hiller S. Regulation of chaperone function by coupled folding and oligomerization. Sci Adv. 2020;6:eabc5822.

Masuda T, Saito N, Tomita M, Ishihama Y. Unbiased quantitation of *Escherichia coli* membrane proteome using phase transfer surfactants. Mol Cell Proteomics. 2009;8:2770–7.

McMorran LM, Bartlett AI, Huysmans GHM, Radford SE, Brockwell DJ. Dissecting the effects of periplasmic chaperones on the in vitro folding of the outer membrane protein PagP. J Mol Biol. 2013;425:3178–91.

Missiakas D, Betton J-M, Raina S. New components of protein folding in extracytoplasmic compartments of *Escherichia coli* SurA, FkpA and Skp/OmpH. Mol Microbiol. 1996;21:871–84.

Mitternacht S. FreeSASA: an open source C library for solvent accessible surface area calculations. F1000Research. 2016;5: 1–11.

Myers JK, Pace CN, Scholtz JM. Denaturant m values and heat capacity changes: relation to changes in accessible surface areas of protein unfolding. Protein Sci. 1995;4:2138–48.

Nakamura K, Mizushima S. Effects of heating in dodecyl sulfate solution on the conformation and electrophoretic mobility of isolated major outer membrane proteins from *Escherichia coli* K-12. J Biochem. 1976;80:1411–22.

Olsson S, Ekonomiuk D, Sgrignani J, Cavalli A. Molecular dynamics of biomolecules through direct analysis of dipolar couplings. J Am Chem Soc. 2015;137:6270–8.

Padiolleau-Lefèvre S, Débat H, Phichith D, Thomas D, Friboulet A, Avalle B. Expression of a functional scFv fragment of an anti-idiotypic antibody with a β-lactam hydrolytic activity. Immunol Lett. 2006;103:39–44.

Pan S, Yang C, Zhao XS. Affinity of Skp to OmpC revealed by single-molecule detection. Sci Rep. 2020;10:1–11.

Philo JS. Improved methods for fitting sedimentation coefficient distributions derived by time-derivative techniques. Anal Biochem. 2006;354:238–46.

Plummer AM, Fleming KG. BamA alone accelerates outer membrane protein folding in vitro through a catalytic mechanism. Biochemistry. 2015;54:6009–11.

Plummer AM, Fleming KG. From chaperones to the membrane with a BAM! Trends Biochem Sci. 2016;41:872–82.

Pocanschi CL, Apell HJ, Puntervoll P, Høgh B, Jensen HB, Welte W, et al. The major outer membrane protein of *Fusobacterium nucleatum* (FomA) folds and inserts into lipid bilayers via parallel folding pathways. J Mol Biol. 2006;355:548–61.

Qu J, Mayer C, Behrens S, Holst O, Kleinschmidt JH. The trimeric periplasmic chaperone Skp of *Escherichia coli* forms 1:1 complexes with outer membrane proteins via hydrophobic and electrostatic interactions. J Mol Biol. 2007;374:91–105.

Ramm K, Plückthun A. The periplasmic Escherichia coli peptidyl-prolyl cis,trans-isomerase FkpA II. Isomerase-independent chaperone activity in vitro. J Biol Chem. 2000;275:17106–13.

Ramm K, Plückthun A. High enzymatic activity and chaperone function are mechanistically related features of the dimeric E. coli peptidyl-prolyl isomerase FkpA. J Mol Biol. 2001;310:485–98.

Rhodius VA, Suh WC, Nonaka G, West J, Gross CA. Conserved and variable functions of the σ^E stress response in related genomes. PLoS Biol. 2006;4:43–0059.

Ruiz-Perez F, Henderson IR, Nataro JP. Interaction of FkpA, a peptidyl-prolyl *cis/trans* isomerase with EspP autotransporter protein. Gut Microbes. 2010;1:339–44.

Sandlin CW, Zaccai NR, Fleming KG. Skp trimer formation is insensitive to salts in the physiological range. Biochemistry. 2015;54:7059–62.

Saul FA, Arié JP, Vulliez-le Normand B, Kahn R, Betton JM, Bentley GA. Structural and functional studies of FkpA from *Escherichia coli*, a *cis/trans* peptidyl-prolyl isomerase with chaperone activity. J Mol Biol. 2004;335:595–608.

Schiffrin B, Calabrese AN, Higgins AJ, Humes JR, Ashcroft AE, Kalli AC, et al. Effects of periplasmic chaperones and membrane thickness on BamA-catalyzed outer-membrane protein folding. J Mol Biol. 2017;429:3776–92.

Schiffrin B, Machin JM, Karamanos TK, Zhuravleva A, Brockwell DJ, Radford SE, et al. Dynamic interplay between the periplasmic chaperone SurA and the BAM complex in outer membrane protein folding. Commun Biol. 2022;5:1–15.

Silhavy TJ, Ruiz N, Kahne D. Advances in understanding bacterial outer-membrane biogenesis. Nat Rev Microbiol. 2006;4:57–66.

Sklar JG, Wu T, Kahne D, Silhavy TJ. Defining the roles of the periplasmic chaperones SurA, Skp, and DegP in *Escherichia coli*. Genes Dev. 2007;21:2473–84.

Soltes GR, Schwalm J, Ricci DP, Silhavy TJ. The activity of *Escherichia coli* chaperone SurA is regulated by conformational changes involving a parvulin domain. J Bacteriol. 2016;198:921–9.

Stafford WF, Sherwood PJ. Analysis of heterologous interacting systems by sedimentation velocity: curve fitting algorithms for estimation of sedimentation coefficients, equilibrium and kinetic constants. Biophys Chem. 2004;108:231–43.

Surrey T, Jahnig F. Kinetics of folding and membrane insertion of a β-barrel membrane protein. J Biol Chem. 1995;270:28199–203.

Tan AE, Burgess NK, DeAndrade DS, Marold JD, Fleming KG. Self-association of unfolded outer membrane proteins. Macromol Biosci. 2010;10:763–7.

Thoma J, Burmann BM, Hiller S, Müller DJ. Impact of holdase chaperones Skp and SurA on the folding of β-barrel outer-membrane proteins. Nat Struct Mol Biol. 2015;22:795–802.

Walton TA, Sandoval CM, Fowler CA, Pardi A, Sousa MC. The cavity-chaperone Skp protects its substrate from aggregation but allows independent folding of substrate domains. Proc Natl Acad Sci U S A. 2009;106:1772–7.

Walton TA, Sousa MC. Crystal structure of Skp, a prefoldin-like chaperone that protects soluble and membrane proteins from aggregation. Mol Cell. 2004;15:367–74.

Wang H, Andersen KK, Vad BS, Otzen DE. OmpA can form folded and unfolded oligomers. Biochim Biophys Acta - Proteins Proteomics. 2013;1834:127–36.

Wu R, Bakelar JW, Lundquist K, Zhang Z, Kuo KM, Ryoo D, et al. Plasticity within the barrel domain of BamA mediates a hybrid-barrel mechanism by BAM. Nat Commun. 2021;12:1–16.

Wu S, Ge X, Lv Z, Zhi Z, Chang Z, Zhao XS. Interaction between bacterial outer membrane proteins and periplasmic quality control factors: a kinetic partitioning mechanism. Biochem J. 2011; 438:505–11.

Wülfing C, Plückthun A. Protein folding in the periplasm of *Escherichia coli*. Mol Microbiol. 1994;12:685–92.

Zaccai NR, Sandlin CW, Hoopes JT, Curtis JE, Fleming PJ, Fleming KG, et al. Deuterium labeling together with contrast variation small-angle neutron scattering suggests how Skp captures and releases unfolded outer membrane proteins. Methods in enzymology. 2016;566:159–210.

SUPPORTING INFORMATION

Additional supporting information can be found online in the Supporting Information section at the end of this article.

How to cite this article: Devlin T, Marx DC, Roskopf MA, Bubb QR, Plummer AM, Fleming KG. FkpA enhances membrane protein folding using an extensive interaction surface. Protein Science. 2023;32(4):e4592. https://doi.org/10.1002/pro.4592